DALTON
FULL PAPER

Theoretical study on linear dicyanide and dicarbonyl complexes of the metals Au, Hg, and Tl. On the possible existence of a $[Tl(CO)_2]^{3+}$ cation §

Volker Jonas † and Walter Thiel *‡

Organisch-Chemisches Institut, Universität Zürich, Winterthurerstrasse 190, CH-8057 Zürich, Switzerland

Received 14th June 1999, Accepted 6th September 1999

DFT-BP86, MP2, and CCSD(T) calculations on the cyanide complexes $[Au(CN)_2]^-$, $[Hg(CN)_2]$, and $[Tl(CN)_2]^+$ and the isoelectronic carbonyl complexes $[Au(CO)_2]^+$, $[Hg(CO)_2]^{2+}$, and $[Tl(CO)_2]^{3+}$ are presented using effective core potential wavefunctions in conjunction with polarized double- and triple-zeta basis sets. Geometries, vibrational frequencies, infrared intensities, internal force fields, and charge distributions are discussed. For the Au and Hg systems, the calculated data are in very good agreement with experimental data. For the complexes $[Tl(CO)_2]^{3+}$ and $[Tl(CN)_2]^+$, the calculations predict metal–C force constants comparable to those in the respective Hg species. The dissociation of these complexes into Tl^+ and CO^+ or CN is computed to be endothermic by about 60 kcal mol^{-1} for $[Tl(CN)_2]^+$ and exothermic by more than 200 kcal mol^{-1} for $[Tl(CO)_2]^{3+}$, with a barrier of 15–20 kcal mol^{-1} (UBP86) in the latter case.

Introduction

In the last few years, the interest in homoleptic transition metal carbonyl cations has increased dramatically with the synthesis of new highly charged species. These include the trication $[Ir(CO)_6]^{3+}$,[1] the dications $[M(CO)_6]^{2+}$ (M = Fe,[2a,b] Ru,[2c] Os[2c]), $[M(CO)_4]^{2+}$ (M = Pd, Pt),[3] $[Pd_2(CO)_2]^{2+}$,[4] and $[Hg_m(CO)_2]^{2+}$ (m = 1, 2),[5] and the monocations $[Cu(CO)_m]^+$ (m = 1–4),[6–8] $[Ag(CO)_m]^+$ (m = 1–4),[7–9] and $[Au(CO)_m]^+$ (m = 1–3).[8,10] The work on homoleptic carbonyl cations of electron-rich metals has been reviewed recently.[11–13]

Several series of homoleptic transition metal carbonyl cations may be distinguished: (a) octahedral hexacarbonyl d^6 ions $[M(CO)_6]^n$ which have been characterized experimentally (M = Mn, Re, Fe, Ru, Os, Ir)[1,2,14] and theoretically;[15–17] (b) square planar tetracarbonyl d^8 ions $[M(CO)_4]^n$ including the dications[3,18] $[Pd(CO)_4]^{2+}$ and $[Pt(CO)_4]^{2+}$ as well as the monocations[18] $[Rh(CO)_4]^+$ and $[Ir(CO)_4]^+$; (c) the d^{10} ions $[M(CO)_m]^+$ which are known[6–10,19] for M = Cu, Ag (m = 1–4) and M = Au (m = 1–3). $[Hg(CO)_2]^{2+}$ is the only corresponding Group 12 species that has been characterized.[5,19]

We have established that density functional calculations of vibrational spectra are reliable for neutral transition metal carbonyls,[20] carbonyl hydrides,[21] charged octahedral hexacarbonyls $[M(CO)_6]^n$,[15] and charged square planar tetracarbonyls.[18] The calculated symmetry force fields for the different carbonyl complexes have been discussed elsewhere in some detail.[22]

In this paper, we present geometries, harmonic frequencies, IR intensities, and force constants for the d^{10} carbonyl cations $[M(CO)_2]^n$ (M = Au, Hg, Tl; n = 1 to 3, respectively) and the isoelectronic cyanide complexes $[M(CN)_2]^n$ (M = Au, Hg, Tl; n = −1 to 1, respectively). Both $[Au(CN)_2]^-$ and $[Hg(CN)_2]$ are well known, and the vibrational spectra of several $[Au(CN)_2]^-$ salts and neutral $[Hg(CN)_2]$ have been extensively investigated from the 1950's to the 1970's.[23–27] The homologous $[Tl(CN)_2]^+$ cation has been observed in aqueous solution as a hydrated, probably octahedral $[Tl(CN)_2(OH_2)_4]^+$ species.[28] Previous theoretical work has focused on the bonding in $[Hg(CN)_2]$ and $[Tl(CN)_2]^+$,[29] and on the structures, energetics and vibrational spectra of the homologous $[Ag(CX)_2]^n$ and $[Au(CX)_2]^n$ (X = N, O; n = −1, +1, respectively) compounds.[30] Calculations on the ^{13}C chemical shifts have also been done,[31] but the vibrational spectra of the Hg and Tl complexes and the force constants of all systems considered have not yet been studied theoretically in the published literature.

The discussion of the present results will emphasize systematic trends within the two series of isoelectronic and isostructural molecules, particularly with regard to the force constants which provide detailed information on the bonding in these complexes. In addition, we address the thermodynamic and kinetic stability of the yet unknown $[Tl(CO)_2]^{3+}$ cation.

Computational details

The quantum chemical calculations were carried out at three different levels of theory, *i.e.* gradient corrected DFT,[32,33] MP2,[34] and CCSD(T).[35] For the DFT calculations, gradient corrections for exchange and for correlation were taken from the work of Becke[32] and Perdew,[33] respectively (usually abbreviated as BP or BP86). Two basis sets were employed, labelled ECP1 and ECP2. For Au and Hg both use a quasi-relativistic effective core potential (ECP) at the transition metal together with the corresponding (8s7p5d)/[6s5p3d] valence basis set.[36] Tl is described by the recently published analogous 21 valence-electron ECP together with a (11s11p8d)/[6s6p4d] valence basis set.[37] For carbon, nitrogen and oxygen, ECP1 employs the 6-31G(d) basis,[38] whereas ECP2 uses a Dunning (10s6p)/[5s3p] triple-zeta basis[39] supplemented by two sets of d

† *Present address*: San Diego Supercomputer Center, 9500 Gilman Drive, San Diego CA 92093-0505, USA. E-mail: vjonas@sdsc.edu
‡ *New address*: Max-Planck Institut für Kohlenforschung, Kaiser-Wilhelm-Platz 1, D-45470 Mülheim an der Ruhr, Germany. E-mail: thiel@mpi-muelheim.mpg.de
§ *Supplementary data available*: calculated bond lengths (ECP1), calculated vibrational frequencies (EPC1), calculated IR intensities (ECP1), experimental and calculated Raman intensities (BP86/ECP2), experimental and calculated isotopic shifts, and calculated symmetry force constants (ECP2). For direct electronic access see http://www.rsc.org/suppdata/dt/1999/3783/, otherwise available from BLDSC (No. SUP 57640, 10 pp.) or the RSC Library. See Instructions for Authors, 1999, Issue 1 (http://www.rsc.org/dalton).

Table 1 Experimental and calculated bond lengths (in Å) for $[Au(CN)_2]^-$, $[Hg(CN)_2]$, $[Tl(CN)_2]^+$, $[Au(CO)_2]^+$, $[Hg(CO)_2]^{2+}$ and $[Tl(CO)_2]^{3+}$

	$[Au(CN)_2]^-$		$[Hg(CN)_2]$		$[Tl(CN)_2]^+$	
	Au–C	C–N	Hg–C	C–N	Tl–C	C–N
Exp.	2.019(12)[a]	1.106(14)[a]	2.015(3)[d]	1.137(3)[d]	[e]	
	1.979(12)[b]	1.167(16)[b]				
	1.982(19)[c]	1.123(27)[c]				
BP86/ECP2	2.002	1.173	2.023	1.166	2.045	1.168
MP2/ECP2	1.992	1.176	2.009	1.171	2.013	1.175
CCSD(T)/ECP2	2.012	1.169	2.024	1.164	2.028	1.166
	$[Au(CO)_2]^+$		$[Hg(CO)_2]^{2+}$		$[Tl(CO)_2]^{3+}$	
	Au–C	C–O	Hg–C	C–O	Tl–C	C–O
Exp.			2.083(10)[f]	1.104(12)[f]		
BP86/ECP2	1.990	1.128	2.116	1.120	2.244	1.121
MP2/ECP2	1.994	1.127	2.109	1.124	2.175	1.128
CCSD(T)/ECP2	2.016	1.122	2.130	1.116	2.203	1.117

[a] Ref. 45(*a*), average values for [LysH][Au(CN)$_2$]. Specific values: Au–C^1 2.022(12) Å, Au–C^2 2.015(12) Å; C^1–N^1 1.100(14) Å, C^2–N^2 1.112(14) Å. [b] Ref. 45(*b*), values for [2,7-bis(methylseleno)-1,6-dithiapyrene]dicyanogold. [c] Ref. 45(*c*), values for [Au{(Ph$_2$PCH$_2$)$_2$AsPh}$_2$][Au(CN)$_2$]. [d] Ref. 46, values corrected for thermal motion are: Hg–C 2.019(3) Å, C–N 1.160(3) Å. [e] Ref. 28(*c*) gives a value of 2.11(2) Å; for *trans*-$[Tl(CN)_2(OH_2)_4]^+$ in aqueous solution, obtained from large-angle X-ray scattering. [f] Ref. 5(*b*), values for $[Hg(CO)_2][Sb_2F_{11}]_2$.

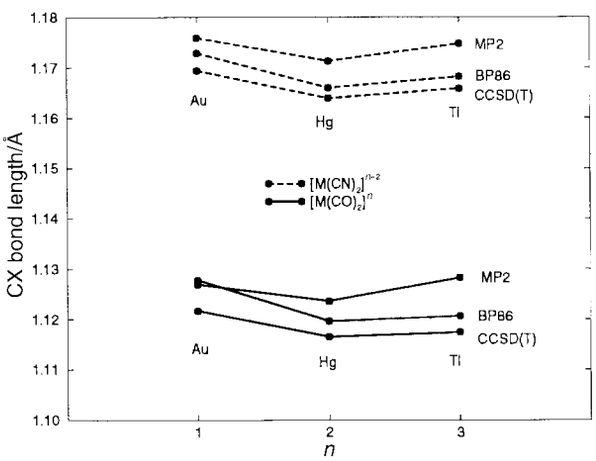

Fig. 1 CX bond lengths (in Å) *versus* total charge *n* for $[M(CO)_2]^n$ and $[M(CN)_2]^{n-2}$ (X = N, O, respectively).

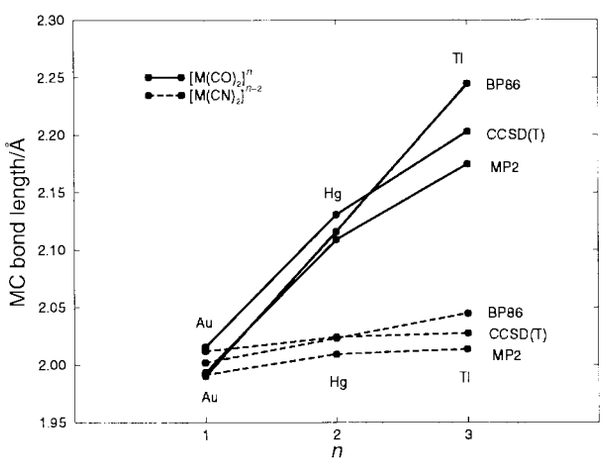

Fig. 2 MC bond lengths (in Å) *versus* total charge *n* for $[M(CO)_2]^n$ and $[M(CN)_2]^{n-2}$.

polarization functions.[40] Spherical d functions were used throughout.

The DFT and MP2 calculations were done with the GAUSSIAN94 and GAUSSIAN98 program systems,[41,42] whereas the CCSD(T) calculations were carried out with the program ACES II.[43] Molecular geometries were optimized within the constraint of $D_{\infty h}$ point group symmetry using analytic energy gradients. Second derivatives were obtained by numerical differentiation of the analytic energy gradients with GAUSSIAN94 and ACES II and analytically with GAUSSIAN98 for the BP86 calculations, which also provides Raman intensities at this level of theory. The force field transformations into internal and symmetry coordinates were performed with the program INTDER.[44] All force constants are given in mdyn Å^{-1} for stretches and stretch–stretch interactions, and mdyn Å rad^{-2} for bends and bend–bend interactions.

Results

General aspects

Throughout this paper, we report BP86/ECP2, MP2/ECP2, and CCSD(T)/ECP2 data which are available for all complexes and should generally be more reliable than the respective ECP1 data due to the use of a larger basis set. To keep the Tables in this paper as short as possible, all ECP1 results were put into the Supplementary Material (Tables S1–S4), and only the ECP2 results are discussed. In addition, the Supplementary Material documents the BP86/ECP2 results for Raman intensities, isotopic shifts, and symmetry force constants (Tables S5–S8).

In the case of transition metal carbonyl and cyanide complexes, only the anharmonic frequencies are generally available from experiment. Since anharmonicity effects normally lower the vibrational frequencies (*e.g.* by 27 cm^{-1} for free CO), the computed harmonic frequencies and the associate force constants should tend to be higher than the observed frequencies and the effective force constants derived therefrom. However, as the overall agreement between experimental (anharmonic) and calculated (harmonic) frequencies has generally been quite good in our previous studies[15,20,21] without correcting for anharmonicity effects, we expect a similar accuracy herein.

Molecular geometries

Table 1 lists the calculated bond lengths for the linear dicyanide complexes and dicarbonyl ions at BP86/ECP2, MP2/ECP2, and CCSD(T)/ECP2 together with the available experimental data. Fig. 1 and 2 display the calculated bond lengths from Table 1.

The calculated bond lengths on all levels are in good agreement with the experimental data from several X-ray structural

Table 2 Vibrational frequencies (in cm^{-1}) for $[Au(CN)_2]^-$, $[Hg(CN)_2]$ and $[Tl(CN)_2]^+$

			Exp. ν_i [a–c] (solution)	BP86 ECP2	$\Delta\nu$	MP2 ECP2	$\Delta\nu$	CCSD(T) ECP2	$\Delta\nu$
		$[Au(CN)_2]^-$							
Σ_g^+	ν_1	[CN]	2161	2155	−6	2103	−58	2183	+22
Σ_g^+	ν_2	[MC]	446	428	−18	444	−2	427	−19
Σ_u^+	ν_3	[CN]	2142	2139	−3	2089	−53	2169	+27
Σ_u^+	ν_4	[MC]	426	407	−19	416	−10	402	−24
Π_g	ν_5	[δMCN]	301	283	−18	297	−4	292	−9
Π_u	ν_6	[δMCN]	410	411	+1	407	−3	397	−13
Π_u	ν_7	[δCMC]	125	77	−48	73	−52	72	−53
		$[Hg(CN)_2]$							
Σ_g^+	ν_1	[CN]	2197	2209	+12	2129	−68	2224	+27
Σ_g^+	ν_2	[MC]	412	417	+5	445	+33	435	+23
Σ_u^+	ν_3	[CN]	2197	2209	+12	2127	−70	2221	+24
Σ_u^+	ν_4	[MC]	442	451	+9	469	+27	458	+16
Π_g	ν_5	[δMCN]	276	233	−43	241	−35	238	−38
Π_u	ν_6	[δMCN]	341	344	+3	332	−9	327	−14
Π_u	ν_7	[δCMC]		74		70		69	
		$[Tl(CN)_2]^+$							
Σ_g^+	ν_1	[CN]	2187	2192	+5	2094	−93	2205	+18
Σ_g^+	ν_2	[MC]	390	388	−2	449	+59	436	+46
Σ_u^+	ν_3	[CN]	2199	2197	−2	2093	−106	2204	+5
Σ_u^+	ν_4	[MC]	345 [d]	475		509		497	
Π_g	ν_5	[δMCN]		194		199		195	
Π_u	ν_6	[δMCN]		293		291		286	
Π_u	ν_7	[δCMC]		65		64		63	

[a] Solution values for $K[Au(CN)_2]$, ref. 24. IR data from 1-methyl-2-pyrrolidone solution; Raman data from aqueous solution. [b] Ref. 23, 26, 27 for $[Hg(CN)_2]$. IR values from solid state (mineral oil mull); Raman values from aqueous solution. [c] Ref. 28(*c*) for $[Tl(CN)_2]^+$. IR and Raman data in aqueous solution, bands attributed to *trans*-$[Tl(CN)_2(OH_2)_4]^+$. [d] Assignment inconsistent with present theoretical results.

analyses of $[Au(CN)_2]^-$ salts,[45] the neutron diffraction data for $[Hg(CN)_2]$,[46] and the X-ray data for $[Hg(CO)_2]^{2+}$.[5b] For the $[Au(CN)_2]^-$ ion, many experimental crystal structures with different counter cations are known in the literature. For comparison with our calculated results, we have chosen some of the newer data including large cations which should distort the anion only to a small extent (see Table 1).[45] In the experimental structure determination of $[Hg(CO)_2]^{2+}$, secondary contacts with the $[Sb_2F_{11}]^-$ counter anion have been observed, which may be the reason for the deviation of *ca.* 0.03 Å between the experimental and calculated Hg–C bond length.[5b]

Within the three levels of theory, some interesting trends can be observed (see Fig. 1 and 2): in five out of six cases, MP2/ECP2 gives the shortest M–C bond and the longest C–X bond, while CCSD(T)/ECP2 always yields the shortest C–X bond lengths. The MP2 and CCSD(T) values show parallel trends for both series, whereas the BP86 bond lengths vary more strongly. For the $[M(CN)_2]^n$ series, the increase of the M–C bond lengths is much smaller than for the $[M(CO)_2]^n$ series, such that the M–C bond is of comparable length in $[Tl(CN)_2]^+$ and $[Hg(CN)_2]$, but much longer in $[Tl(CO)_2]^{3+}$ than in $[Hg(CO)_2]^{2+}$.

Vibrational frequencies

For linear $[M(CX)_2]^n$, the vibrational representation reduces as follows:

$$\Gamma_{vib} = 2\,\Sigma_g^+ + 2\,\Sigma_u^+ + \Pi_g + 2\,\Pi_u$$

Table 2 contains the calculated vibrational frequencies for the linear dicyanide complexes together with the available experimental data.

Both $[Au(CN)_2]^-$ and $[Hg(CN)_2]$ are long known and their vibrational spectra have been assigned.[24,25] The assignment of fundamentals for $[Au(CN)_2]^-$ follows the work of Willner[10b] with the experimental values for $K[Au(CN)_2]$ in solution taken from the work of Chadwick and Frankiss.[24a] We assign the weak shoulder at 410 cm^{-1} in the infrared to ν_6,[24a] which is supported by the calculated low intensity (see Table 4 below). In general, our calculated BP86/ECP2 frequencies are in good agreement with the experimental data except for ν_7. Similar to the highly charged carbonyl cations,[15,47] the experimental value for this C–M–C bending vibration is much higher than the calculated value, probably due to counter ion or solid state effects.

Within the three levels of theory employed, the BP86 results show the best agreement with the experimental data. At MP2/ECP2, ν_1 and ν_3 are calculated much too low (−58 and −53 cm^{-1}, respectively), most probably due to the overestimated C–N bond length. At CCSD(T)/ECP2, both values are too high by +22 and +27 cm^{-1}, respectively. For the other vibrations, the differences between the three levels are not very large (Table 2). The experimental splitting of ν_1 and ν_3 (19 cm^{-1}) is slightly higher than computed: BP86 gives 16 cm^{-1}, whereas MP2 and CCSD(T) give 14 cm^{-1}.

The assignment of the vibrational frequencies of $[Hg(CN)_2]$ follows the work of Jones.[23,25] At BP86/ECP2, the deviations are somewhat higher than for $[Au(CN)_2]^-$ with +12 cm^{-1} for ν_1 and ν_3. Analogous to $[Au(CN)_2]^-$, ν_1 and ν_3 are calculated much too low at MP2/ECP2 and too high at CCSD(T)/ECP2 (Table 2). The splitting between ν_1 and ν_3 is small (*i.e.* less than 1 cm^{-1} experimentally[25] and at BP86/ECP2, 2 cm^{-1} at MP2/ECP2 and 3 cm^{-1} at CCSD(T)/ECP2).

Table 2 also lists the calculated vibrational frequencies for $[Tl(CN)_2]^+$. The BP86 values for both CN stretching frequencies (ν_1, ν_3) and for the symmetric TlC stretching frequency (ν_2) are in excellent agreement with the available experimental values for *trans*-$[Tl(CN)_2(OH_2)_4]^+$;[28c] however, for the antisymmetric Tl–C stretching frequency (ν_4), there is such a large discrepancy that we suspect a misassignment.[28c] The BP86 data are generally quite close to the CCSD(T) data and may thus serve as predictions for the remaining bands.

Table 3 contains the vibrational frequencies for the $[M(CO)_2]^n$ series together with the experimental data for the Au and Hg compounds.

Table 3 Vibrational frequencies (in cm^{-1}) for $[Au(CO)_2]^+$, $[Hg(CO)_2]^{2+}$ and $[Tl(CO)_2]^{3+}$

			Exp. ν_i [a,b] (soid)	BP86 ECP2	$\Delta\nu$	MP2 ECP2	$\Delta\nu$	CCSD(T) ECP2	$\Delta\nu$
		$[Au(CO)_2]^+$							
Σ_g^+	ν_1	[CO]	2254	2238	−16	2220	−34	2280	+26
Σ_g^+	ν_2	[MC]	400	405	+5	398	−2	378	−22
Σ_u^+	ν_3	[CO]	2217	2197	−20	2190	−27	2250	+33
Σ_u^+	ν_4	[MC]	354	359	+5	344	−10	331	−23
Π_g	ν_5	[δMCO]	312	298	−14	318	+6	310	−2
Π_u	ν_6	[δMCO]	406	397	−9	401	−5	391	−15
Π_u	ν_7	[δCMC]	105	59	−46	54	−51	53	−52
		$[Hg(CO)_2]^{2+}$							
Σ_g^+	ν_1	[CO]	2281	2287	+6	2214	−67	2306	+25
Σ_g^+	ν_2	[MC]		320		333		320	
Σ_u^+	ν_3	[CO]	2278	2283	+5	2214	−64	2303	+25
Σ_u^+	ν_4	[MC]		349		362		349	
Π_g	ν_5	[δMCO]		277		289		285	
Π_u	ν_6	[δMCO]	335	341	+6	336	+1	328	−7
Π_u	ν_7	[δCMC]		64		58		56	
		$[Tl(CO)_2]^{3+}$							
Σ_g^+	ν_1	[CO]		2264		2138		2279	
Σ_g^+	ν_2	[MC]		253		327		305	
Σ_u^+	ν_3	[CO]		2266		2140		2279	
Σ_u^+	ν_4	[MC]		327		381		358	
Π_g	ν_5	[δMCO]		271		287		283	
Π_u	ν_6	[δMCO]		312		325		318	
Π_u	ν_7	[δCMC]		60		60		58	

[a] Ref. 10(*b*); values for solid $[Au(CO)_2][Sb_2F_{11}]$. [b] Ref. 5(*b*); values for solid $[Hg(CO)_2][Sb_2F_{11}]_2$.

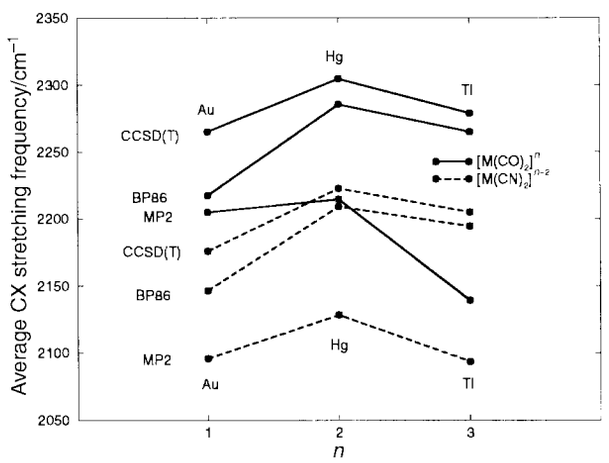

Fig. 3 Average CX stretching frequencies (in cm^{-1}) *versus* total charge *n* for $[M(CO)_2]^n$ and $[M(CN)_2]^{n-2}$ (X = N, O, respectively).

Both $[Au(CO)_2]^+$ and $[Hg(CO)_2]^{2+}$ have been synthesized as their respective $[Sb_2F_{11}]^-$ salts and the vibrational spectra of the solids have been assigned.[5b,10b] For $[Au(CO)_2]^+$, complete experimental vibrational data are available, whereas for $[Hg(CO)_2]^{2+}$ only the two C–O bands have been assigned; there are three medium IR bands at 335 cm^{-1}, 325 cm^{-1} and 311 cm^{-1} which may be assigned to ν_4 and ν_6 (see Table 4 below), but which may also originate from the $[Sb_2F_{11}]^-$ counter anion.[5b] Analogous to other solid state spectra and as for $[Au(CN)_2]^-$, the deviation for the C–M–C bending vibration ν_7 is rather large in $[Au(CO)_2]^+$. In an overall comparison, the BP86/ECP2 results are closest to the available experimental data (Table 3). It should be noted, however, that this assessment neglects anharmonicity effects (see above). If such effects were taken into account for the CO stretching modes (*ca.* −27 cm^{-1} as in free CO), CCSD(T)/ECP2 would be superior to BP86/ECP2 while the errors for MP2/ECP2 would increase still further (Table 3).

Fig. 3 compares the calculated average C–X (X = O, N) vibrational frequencies at the three levels employed in this study for the linear dicarbonyl ions and dicyanide complexes. Obviously the CCSD(T) values are consistently higher than the BP86 values, but show the same trends. On the other hand, the MP2 frequencies are always much lower and look less systematic, especially for the CO complexes. We conclude from these comparisons (Tables 2, 3 and Fig. 3) that both BP86 and CCSD(T) describe these molecules well, whereas MP2 has severe difficulties, particularly with the highly charged cations.

Infrared intensities

Table 4 contains the calculated infrared intensities for the linear dicarbonyl ions and dicyanide complexes together with the available spectroscopic data for the Au and Hg systems.

The calculated intensities nicely reproduce the trends found experimentally for the Au and Hg systems with the exception of $[Au(CO)_2]^+$ (see below). The highest absolute IR intensities are calculated for the monocations $[Au(CO)_2]^+$ and $[Tl(CN)_2]^+$. The trend towards lower IR intensities for highly charged cations has also been found for the hexacarbonyl and tetracarbonyl series.[15,18] For each molecule, the calculated infrared intensities at the three levels are very similar. The main difference between the cyanide and CO complexes can be seen for ν_4 and ν_6: for all cyanide complexes and also $[Au(CO)_2]^+$, ν_4 is much stronger than ν_6, whereas for the highly charged $[Hg(CO)_2]^{2+}$ and $[Tl(CO)_2]^{3+}$ this trend is opposite with the calculated intensities for ν_4 close to zero.

For $[Au(CO)_2]^+$, the experimental IR intensities for ν_4 and ν_6 are quite sensitive to the medium where the spectra are taken: solid $[Au(CO)_2][Sb_2F_{11}]$[10b] ν_4 at 354 cm^{-1} (w) and ν_6 at 406 cm^{-1} (m); solid $[Au(CO)_2][UF_6]$[47] ν_4 at 349 cm^{-1} (m) and ν_6 at 398 cm^{-1} (m) with nearly equal intensity; in HSO_3F solution,[10b] ν_4 at 352 cm^{-1} (w) and no band around 406 cm^{-1}. In view of these conflicting experimental data, a conclusive assessment is only possible with the help of isotopic shifts: the assignment of ν_4 at 354 cm^{-1} and ν_6 at 406 cm^{-1} is strongly supported by the excellent agreement between the observed[22] and calculated isotopic shifts (see Table S6).

Table 4 Experimental relative and calculated infrared intensities (in km mol^{-1}) for $[Au(CN)_2]^-$, $[Hg(CN)_2]$, $[Tl(CN)_2]^+$, $[Au(CO)_2]^+$, $[Hg(CO)_2]^{2+}$ and $[Tl(CO)_2]^{3+}$ [a]

			Exp.[b]	BP86	MP2	CCSD(T)	Exp.[c]	BP86	MP2	CCSD(T)
			$[Au(CN)_2]^-$				$[Au(CO)_2]^+$			
Σ_u^+	ν_3	[CX]	s	75.3	23.7	36.5	s	499.7	256.1	332.7
Σ_u^+	ν_4	[MC]	m	15.6	11.0	16.3	w[d]	49.5	57.4	44.5
Π_u	ν_6	[δMCX]	sh	0.3	0.0	0.1	m[d]	10.1	5.4	9.3
Π_u	ν_7	[δCMC]	m,bd	35.3	35.3	36.5	vw	0.5	0.7	0.5
			$[Hg(CN)_2]$				$[Hg(CO)_2]^{2+}$			
Σ_u^+	ν_3	[CX]	vs	50.3	78.8	57.1	m	15.6	6.6	2.7
Σ_u^+	ν_4	[MC]	s	43.4	44.1	47.2		0.9	0.0	0.0
Π_u	ν_6	[δMCX]	m	0.2	0.9	0.8	m	21.1	10.6	14.6
Π_u	ν_7	[δCMC]		23.8	27.9	28.0		3.1	2.7	2.2
			$[Tl(CN)_2]^+$				$[Tl(CO)_2]^{3+}$			
Σ_u^+	ν_3	[CX]		319.0	340.3	320.3		26.0	143.0	33.8
Σ_u^+	ν_4	[MC]		26.8	35.2	35.5		3.5	0.0	0.4
Π_u	ν_6	[δMCX]		1.1	2.5	3.1		29.1	14.6	20.1
Π_u	ν_7	[δCMC]		10.1	15.7	14.8		8.2	5.8	5.1

[a] All calculated data were obtained from the ECP2 calculations; X = O or N, respectively. [b] Ref. 24 for $[Au(CN)_2]^-$; ref. 26 for $[Hg(CN)_2]$. [c] Ref. 10(*b*) for $[Au(CO)_2]^+$; ref. 5(*b*) for $[Hg(CO)_2]^{2+}$. [d] See the text.

Table 5 Internal force constants F_{int} for $[Au(CN)_2]^-$, $[Hg(CN)_2]$ and $[Tl(CN)_2]^+$ [a]

	$[Au(CN)_2]^-$				$[Hg(CN)_2]$				$[Tl(CN)_2]^+$		
	Exp.[b]	BP86	MP2	CCSD(T)	Exp.[c]	BP86	MP2	CCSD(T)	BP86	MP2	CCSD(T)
F_{CN}	17.64 ± 0.18	17.02	16.04	17.34	18.07 ± 0.2	17.74	16.24	17.82	17.43	15.50	17.39
F_{MC}	2.78 ± 0.03	2.49	2.67	2.47	2.59 ± 0.03	2.69	3.03	2.88	2.66	3.37	3.16
$F_{CN,CN'}$	0.03 ± 0.18	0.02	0.00	0.02	0.0 ± 0.2	−0.01	−0.02	0.00	−0.01	−0.01	0.00
$F_{MC,MC'}$	0.416 ± 0.025	0.43	0.50	0.45	0.12 ± 0.02	0.10	0.20	0.19	−0.24	−0.04	−0.05
$F_{CN,MC}$	0.3 ± 0.15	0.20	0.11	0.05	0.05 ± 0.15	−0.02	−0.07	−0.11	−0.09	−0.13	−0.14
$F_{CN,MC'}$	0.0 ± 0.15	0.02	0.04	0.03	0.0 ± 0.15	0.01	0.02	0.02	−0.03	−0.03	−0.03
F_β		0.56	0.47	0.45		0.52	0.43	0.41	0.43	0.42	0.39
$F_{\alpha\beta}$		−0.10	−0.09	−0.09		−0.06	−0.05	−0.05	−0.04	−0.04	−0.04
$F_{\alpha\alpha'}$		−0.02	−0.01	−0.01		−0.01	0.00	0.00	−0.01	0.00	0.00
F_α		0.25	0.26	0.26		0.16	0.17	0.17	0.12	0.12	0.11

[a] All calculated data were obtained from the ECP2 calculations. For the notation of force constants see ref. 23, p. 117 ff. See text for units. [b] Ref. 23, 25. [c] Ref. 23, 27; for both molecules the force constants are calculated from the harmonic CN frequencies and observed other frequencies.

Table 6 Internal force constants F_{int} for $[Au(CO)_2]^+$, $[Hg(CO)_2]^{2+}$ and $[Tl(CO)_2]^{3+}$ [a]

	$[Au(CO)_2]^+$				$[Hg(CO)_2]^{2+}$				$[Tl(CO)_2]^{3+}$		
	Exp.[b]	BP86	MP2	CCSD(T)	Exp.	BP86	MP2	CCSD(T)	BP86	MP2	CCSD(T)
F_{CO}	20.1 ± 0.1[c]	19.46	19.16	20.23	20.98[d]	20.49	19.16	20.77	20.17	17.88	20.33
F_{MC}	2.16 ± 0.03	2.24	2.13	1.93		1.68	1.82	1.68	1.26	1.88	1.65
$F_{CO,CO'}$	0.15 ± 0.1	0.05	0.00	0.03		0.00	−0.02	0.00	0.00	−0.03	0.00
$F_{MC,MC'}$	0.54 ± 0.03	0.57	0.59	0.51		0.06	0.07	0.06	−0.17	−0.06	−0.07
$F_{CO,MC}$	0.45 ± 0.2	0.30	0.20	0.13		−0.04	−0.03	−0.10	−0.12	0.02	−0.08
$F_{CO,MC'}$	0.0 ± 0.2	−0.10	−0.06	−0.07		−0.02	0.00	−0.01	−0.04	−0.06	−0.02
F_β	0.77 ± 0.09	0.31	0.25	0.24		0.32	0.23	0.22	0.26	0.25	0.23
$F_{\alpha\beta}$	−0.015 ± 0.015	−0.09	−0.08	−0.08		−0.04	−0.03	−0.03	−0.02	−0.02	−0.02
$F_{\alpha\alpha'}$	0.015 ± 0.02	−0.01	−0.01	−0.01		−0.01	0.00	0.00	0.00	0.00	0.00
F_α	0.268 ± 0.02	0.26	0.29	0.28		0.23	0.24	0.24	0.22	0.24	0.24

[a] All calculated data were obtained from the ECP2 calculations. For the notation of force constants see ref. 23, p. 117 ff. See text for units. [b] Ref. 10(*b*). [c] The experimental value obtained with the Cotton–Kraihanzel method is 20.18 mdyn Å^{-1}, ref. 10(*b*). [d] Ref. 5(*b*); obtained with the Cotton–Kraihanzel method.

Force constants

Tables 5 and 6 contain the calculated internal force constants for the linear dicarbonyl ions and dicyanide complexes together with the available experimental data for the Au and Hg systems.

The corresponding symmetry force constants are only given in the Supplementary Material. Symmetry coordinates have been taken from ref. 23 and are also given in ref. 22. For symmetry reasons, there is no coupling between the four stretching vibrations (ν_1–ν_4) and the three bending vibrations (ν_5–ν_7).

For $[Au(CN)_2]^-$ and $[Hg(CN)_2]$, the internal stretching force constants and coupling elements have been derived from the

Table 7 Atomic charges from natural population analysis[a]

Compound	q_M	q_C	q_X	$q_C + q_X$	$q_C - q_X$
$[Au(CN)_2]^-$	0.30	−0.14	−0.50	−0.65	0.36
$[Hg(CN)_2]$	1.11	−0.25	−0.30	−0.55	0.05
$[Tl(CN)_2]^+$	1.62	−0.24	−0.07	−0.31	−0.18
$[Au(CO)_2]^+$	0.49	0.48	−0.23	0.25	0.72
$[Hg(CO)_2]^{2+}$	1.28	0.47	−0.11	0.36	0.57
$[Tl(CO)_2]^{3+}$	1.84	0.55	0.03	0.58	0.53

[a] BP86/ECP2 values in units of e. M = Au, Hg, or Tl, and X = N or O, respectively. Free CO: q_C 0.46, q_O −0.46, $q_C - q_O$ 0.92. Free CN^-: q_C −0.27, q_N −0.73, $q_C - q_N$ 0.46.

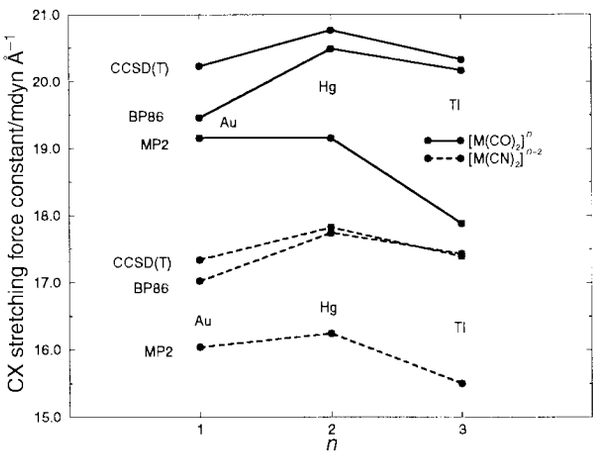

Fig. 4 CX stretching force constants (in mdyn $Å^{-1}$) *versus* total charge *n* for $[M(CO)_2]^n$ and $[M(CN)_2]^{n-2}$ (X = N, O, respectively).

vibrational spectra of isotopic species.[23,25,27] The agreement between the experimental and calculated force constants is satisfactory both for the diagonal and non-diagonal elements. Especially for the non-diagonal coupling elements, BP86 shows the smallest deviations from the experimental values (Table 5).

For $[Au(CO)_2]^+$, the agreement between the experimental and calculated force constants is reasonable for all values except F_β. The overestimation of F_β is a direct consequence of the overestimation of ν_7 (see above). For $[Hg(CO)_2]^{2+}$, no experimental force constants are available except the C–O stretching force constant obtained with the Cotton–Kraihanzel method.[5b,48] The value of 20.98 mdyn $Å^{-1}$ is the highest C–O stretching force constant obtained for a transition metal carbonyl complex so far and nearly approaches the value for HCO^+ (21.3 mdyn $Å^{-1}$).[15]

Charge distributions

Table 7 presents atomic charges obtained from a natural population analysis (NPA)[49] at the BP86/ECP2 level. For both series, the NPA charges behave quite regularly. The charges at carbon are almost constant within each series, whereas oxygen and the metal lose electron density with increasing total charge *n*. Interestingly, NPA predicts a reversal of CN polarity in $[Tl(CN)_2]^+$ relative to $[Hg(CN)_2]$. For the carbonyl series, the calculated partial charges at carbon and oxygen show the same trends as in the $[M(CO)_6]^n$ and $[M(CO)_4]^n$ series:[15,18] for the member with the highest calculated C–O stretching force constant, *i.e.* $[Pt(CO)_6]^{4+}$, $[Au(CO)_4]^{3+}$, and $[Hg(CO)_2]^{2+}$, the calculated NPA charge at oxygen is still negative, and it becomes positive for the next member of each series.

Discussion

In this section, we discuss the variation of the calculated data within the two series $[M(CO)_2]^n$ (3 molecules, total charge *n* between 1 and 3) and $[M(CN)_2]^{n-2}$ (3 molecules, total charge $n - 2$ between −1 and 1). Fig. 4 shows the change in the C–O and C–N stretching force constants F_{CO} and F_{CN} as a function of *n* (Tables 5 and 6). Fig. 5 displays the analogous M–C force constants F_{MC}.

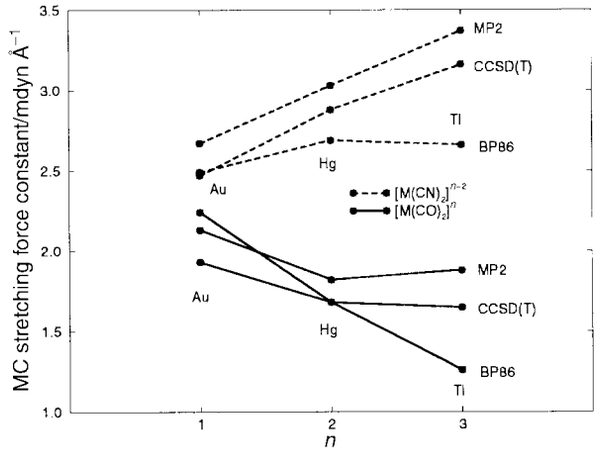

Fig. 5 MC stretching force constants (in mdyn $Å^{-1}$) *versus* total charge *n* for $[M(CO)_2]^n$ and $[M(CN)_2]^{n-2}$.

F_{CO} and F_{CN} increase from M = Au to M = Hg and decrease again to M = Tl. As discussed previously,[15] the upper limit for the C–O stretching force constants should be given by HCO^+ (21.36 mdyn $Å^{-1}$ at BP86/ECP2) where, according to the Dewar–Chatt–Duncanson model,[50] no π backdonation is present. An inverse trend can be seen in the C–O and C–N bond lengths which have the lowest values in each series for the Hg compound (Fig. 1). The trends in Fig. 4 resemble those in Fig. 3, as expected.

The calculated M–C force constants decrease gradually for the $[M(CO)_2]^n$ series with increasing total charge *n*, consistent with the calculated M–C bond lengths (see Fig. 2 and 5) which increase from $[Au(CO)_2]^+$ to $[Hg(CO)_2]^{2+}$ and $[Tl(CO)_2]^{3+}$. However, the trends for the M–C stretching force constants are not entirely uniform (Fig. 5) since the BP86 curve crosses the (almost parallel) MP2 and CCSD(T) curves. This leads to the situation that the M–C force constants for $[Hg(CO)_2]^{2+}$ and $[Tl(CO)_2]^{3+}$ are nearly equal at CCSD(T), while F_{MC} is significantly smaller for $[Tl(CO)_2]^{3+}$ at BP86. In the $[M(CN)_2]^n$ series, there are again some similar differences: the M–C stretching force constant increases in the series M = Au < Hg < Tl for CCSD(T) while it reaches a maximum at M = Hg for BP86 (with M = Tl only slightly lower).

Concerning the coupling force constants (Tables 5 and 6), those involving adjacent bonds ($F_{MC,MC'}$ and $F_{CN,MC}$ or $F_{CO,MC}$) are sizeable for $[Au(CN)_2]^-$ and $[Au(CO)_2]^+$, but become significantly smaller for the Hg and Tl complexes. This may reflect decreasing π backdonation which is at least partly responsible for these interactions. The coupling force constants for non-adjacent bonds ($F_{CN,MC'}$ and $F_{CO,MC'}$) and for different linear bends ($F_{\alpha\beta}$, $F_{\alpha\alpha'}$) are rather small for all complexes considered.

The force constant calculations confirm that $[Tl(CO)_2]^{3+}$ and $[Tl(CN)_2]^+$ are minima on the potential surface, but they provide no evidence on their thermodynamic and kinetic stability. To address this question, we have carried out unrestricted UBP86/ECP2 calculations for the decomposition of these complexes.[51] As expected, the heterolytic dissociation to singlet products is strongly endothermic and will therefore not be

$$[Tl(CO)_2]^{3+} \longrightarrow [Tl(CO)]^{3+} + CO \qquad \Delta E = +127.1 \text{ kcal mol}^{-1} \quad (1)$$

$$[Tl(CO)_2]^{3+} \longrightarrow [Tl(CO)]^{+} + CO^{2+} \qquad \Delta E = +81.4 \text{ kcal mol}^{-1} \quad (2)$$

considered further. The homolytic dissociation into doublet states ($^2\Sigma^+$) is exothermic for $[Tl(CO)_2]^{3+}$ and endothermic for $[Tl(CN)_2]^+$:

$$[Tl(CO)_2]^{3+} \longrightarrow [Tl(CO)]^{2+} + CO^+ \quad \Delta E = -138.4 \text{ kcal mol}^{-1} \quad (3)$$

$$[Tl(CN)_2]^+ \longrightarrow [Tl(CN)]^+ + CN \quad \Delta E = +60.0 \text{ kcal mol}^{-1} \quad (4)$$

Further homolytic dissociation to Tl^+ (closed-shell s^2 configuration) is again exothermic for $[Tl(CO)]^{2+}$ and almost thermoneutral for $[Tl(CN)]^+$:

$$[Tl(CO)]^{2+} \longrightarrow Tl^+ + CO^+ \quad \Delta E = -78.1 \text{ kcal mol}^{-1} \quad (5)$$

$$[Tl(CN)]^+ \longrightarrow Tl^+ + CN \quad \Delta E = +0.3 \text{ kcal mol}^{-1} \quad (6)$$

Similar reaction energies are found at the UBP86/ECP1, UCCSD(T)/ECP1, and UCCSD(T)/ECP2 levels.[52] These thermochemical data clearly show that $[Tl(CN)_2]^+$ is intrinsically quite stable towards unimolecular decomposition while $[Tl(CO)_2]^{3+}$ is thermodynamically unstable.

The barrier for the dissociation reaction (3) has been determined at the unrestricted UBP86/ECP1 and UBP86/ECP2 levels, through reaction coordinate calculations (incrementing one fixed Tl–C distance while optimizing the other coordinates) and subsequent transition state refinement. The computed barriers at these levels are 16.9 and 18.0 kcal mol^{-1}, respectively. The optimized transition structures[53] are fairly unsymmetrical, since the two Tl–C distances differ by 0.65 and 0.69 Å, respectively. It should be noted, however, that the concerted dissociation of both Tl–C bonds in $D_{\infty h}$ symmetry requires only slightly more activation since the corresponding stationary point with two imaginary frequencies lies only about 1.1 kcal mol^{-1} above the unsymmetrical transition state. Inspection of the points on the reaction path shows that there is no spin contamination at the UBP86 level until close to the transition state (*i.e.*, up to a Tl–C elongation of 0.85 Å and a concomitant increase in energy of about 15 kcal mol^{-1}). The spin contamination at the transition state remains minor (S^2 around 0.30 with UBP86[53]).

The dissociation product $[Tl(CO)]^{2+}$ of reaction (3) has a very long Tl–C bond (2.822 Å at UBP86/ECP1 and 2.863 Å at UBP86/ECP2). Reaction coordinate calculations for (5) indicate that this bond can be broken with very little activation. The corresponding transition state is thus mechanistically irrelevant for the overall dissociation process and has therefore not been located. A shallow minimum for $[Tl(CO)]^{2+}$ is also found at UCCSD(T)/ECP1, but not at UCCSD(T)/ECP2, so that it is uncertain whether this monocoordinated complex exists.

The kinetic stability of $[Tl(CO)_2]^{3+}$ is governed by the barrier for step (3). Our best computed UBP86 value of 18 kcal mol^{-1} indicates a reasonable intrinsic stability towards unimolecular decay. On the other hand, this barrier would seem to be rather small compared to the interaction energies with counter ions that will occur in a condensed-phase environment.

Conclusions

The DFT-BP86 and CCSD(T) results for the investigated complexes are generally in good agreement with each other and with the available experimental data (Au and Hg species), whereas MP2 encounters severe difficulties in the case of the highly charged cations. The recently observed $[Tl(CN)_2]^+$ cation is predicted to have similar bond lengths and stretching force constants as the isoelectronic $Hg(CN)_2$ molecule. Likewise, the unknown $[Tl(CO)_2]^{3+}$ cation shows some similarities to the well-characterized $[Hg(CO)_2]^{2+}$ cation. However, in $[Tl(CO)_2]^{3+}$, the Tl–C bond is computed to be quite long, and the dissociation to Tl^+ and 2 CO^+ is found to be strongly exothermic, with a relatively small barrier of 15–20 kcal mol^{-1} (UBP86). Therefore, $[Tl(CO)_2]^{3+}$ is predicted to exist, but it should be difficult to observe this cation experimentally.

Acknowledgements

This work was supported by the Schweizerischer Nationalfonds. The calculations were carried out using IBM RS/6000 and Silicon Graphics workstations at the University Zürich and ETH Zürich (C4 Cluster) as well as the NEC SX-4 computer at CSCS Manno. We thank Dr W. D. Allen, Atlanta, for a copy of the INTDER program.

References

1 C. Bach, H. Willner, C. Wang, S. J. Rettig, J. Trotter and F. Aubke, *Angew. Chem.*, 1996, **108**, 2104; *Angew. Chem., Int. Ed. Engl.*, 1996, **35**, 1974.
2 (*a*) B. Bley, H. Willner and F. Aubke, *Inorg. Chem.*, 1997, **36**, 158; (*b*) E. Bernhardt, B. Bley, R. Wartchow, H. Willner, E. Bill, P. Kuhn, I. H. T. Sham, M. Bodenbinder, R. Bröchler and F. Aubke, *J. Am. Chem. Soc.*, 1999, **121**, 7188; (*c*) C. Wang, B. Bley, G. Balzer-Jöllenbeck, A. R. Lewis, S. C. Siu, H. Willner and F. Aubke, *J. Chem. Soc., Chem. Commun.*, 1995, 2071.
3 G. Hwang, M. Bodenbinder, H. Willner and F. Aubke, *Inorg. Chem.*, 1993, **32**, 4667; (*b*) G. Hwang, C. Wang, F. Aubke, H. Willner and M. Bodenbinder, *Can. J. Chem.*, 1993, **71**, 1532.
4 (*a*) C. Wang, M. Bodenbinder, H. Willner, S. Rettig, J. Trotter and F. Aubke, *Inorg. Chem.*, 1994, **33**, 779; (*b*) C. Wang, S. C. Siu, G. Hwang, C. Bach, B. Bley, M. Bodenbinder, H. Willner and F. Aubke, *Can. J. Chem.*, 1996, **74**, 1952.
5 (*a*) H. Willner, M. Bodenbinder, C. Wang and F. Aubke, *J. Chem. Soc., Chem. Commun.*, 1994, 1189; (*b*) M. Bodenbinder, G. Balzer-Jöllenbeck, H. Willner, R. J. Batchelor, F. W. B. Einstein, C. Wang and F. Aubke, *Inorg. Chem.*, 1996, **35**, 82.
6 (*a*) J. J. Rack, J. D. Webb and S. H. Strauss, *Inorg. Chem.*, 1996, **35**, 277; (*b*) S. M. Ivanova, S. V. Ivanov, S. M. Miller, O. P. Anderson, K. A. Solntsev and S. H. Strauss, *Inorg. Chem.*, 1999, **38**, 3756.
7 F. Meyer, Y.-M. Chen and P. B. Armentrout, *J. Am. Chem. Soc.*, 1995, **117**, 4071.
8 J. J. Rack and S. H. Strauss, *Catal. Today*, 1997, **36**, 99.
9 (*a*) P. K. Hurlburt, J. J. Rack, S. F. Dec, O. P. Anderson and S. H. Strauss, *Inorg. Chem.*, 1993, **32**, 373; (*b*) P. K. Hurlburt, J. J. Rack, J. S. Luck, S. F. Dec, J. D. Webb, O. P. Anderson and S. H. Strauss, *J. Am. Chem. Soc.*, 1994, **116**, 10003.
10 (*a*) H. Willner and F. Aubke, *Inorg. Chem.*, 1990, **29**, 2195; (*b*) H. Willner, J. Schaebs, G. Hwang, F. Mistry, R. Jones, J. Trotter and F. Aubke, *J. Am. Chem. Soc.*, 1992, **114**, 8972.
11 H. Willner and F. Aubke, *Angew. Chem.*, 1997, **109**, 2506; *Angew. Chem., Int. Ed. Engl.*, 1997, **36**, 2402.
12 S. H. Strauss, *Chemtracts: Inorg. Chem.*, 1997, **10**, 77.
13 (*a*) F. Aubke and C. Wang, *Coord. Chem. Rev.*, 1994, **137**, 483; (*b*) L. Weber, *Angew. Chem.*, 1994, **106**, 1131; *Angew. Chem., Int. Ed. Engl.*, 1994, **33**, 1077.
14 (*a*) E. O. Fischer, K. Fichtel and K. Öfele, *Chem. Ber.*, 1962, **95**, 249; (*b*) R. A. N. McLean, *Can. J. Chem.*, 1974, **52**, 213; (*c*) W. Hieber and T. Kruck, *Angew. Chem.*, 1961, **73**, 580; (*d*) W. Hieber and T. Kruck, *Z. Naturforsch., Teil B*, 1961, **16**, 709; (*e*) E. W. Abel, R. A. N. McLean, S. P. Tyfield, P. S. Braterman, A. P. Walker and P. J. Hendra, *J. Mol. Spectrosc.*, 1969, **30**, 29.
15 V. Jonas and W. Thiel, *Organometallics*, 1998, **17**, 353.
16 A. W. Ehlers, Y. Ruiz-Morales, E. J. Baerends and T. Ziegler, *Inorg. Chem.*, 1997, **36**, 5031.
17 R. K. Szilagyi and G. Frenking, *Organometallics*, 1997, **16**, 4807.
18 C. Bach, G. Balzer, H. Willner, F. Aubke, V. Jonas and W. Thiel, to be submitted.
19 A. J. Lupinetti, V. Jonas, W. Thiel, G. Frenking and S. H. Strauss, *Chem. Eur. J.*, 1999, **5**, 2573.
20 V. Jonas and W. Thiel, *J. Chem. Phys.*, 1995, **102**, 8474.
21 V. Jonas and W. Thiel, *J. Chem. Phys.*, 1996, **105**, 3636.
22 V. Jonas and W. Thiel, *J. Phys. Chem. A.*, 1999, **103**, 1381.
23 L. H. Jones, *Inorganic Vibrational Spectroscopy*, Marcel Dekker, New York, 1971.
24 (*a*) B. M. Chadwick and S. G. Frankiss, *J. Mol. Struct.*, 1976, **31**, 1; (*b*) L. H. Jones, *J. Chem. Phys.*, 1957, **27**, 468.
25 L. H. Jones, *J. Chem. Phys.*, 1965, **43**, 594.

26 (*a*) L. H. Jones, *J. Chem. Phys.*, 1957, **27**, 665; (*b*) L. H. Jones, *Spectrochim. Acta*, 1963, **19**, 1675.
27 L. H. Jones, *J. Chem. Phys.*, 1966, **44**, 3643.
28 (*a*) I. Bányai, J. Glaser and J. Losonczi, *Inorg. Chem.*, 1997, **36**, 5900; erratum *Inorg. Chem.*, 1998, **37**, 1135; (*b*) K. E. Berg, J. Blixt and J. Glaser, *Inorg. Chem.*, 1996, **35**, 7074; (*c*) J. Blixt, J. Glaser, J. Mink, I. Persson, P. Persson and M. Sandström, *J. Am. Chem. Soc.*, 1995, **117**, 5089; (*d*) J. Blixt, B. Györi and J. Glaser, *J. Am. Chem. Soc.*, 1989, **111**, 7784.
29 R. Åkesson, I. Persson, M. Sandström and U. Wahlgren, *Inorg. Chem.*, 1994, **33**, 3715.
30 A. Veldkamp and G. Frenking, *Organometallics*, 1993, **12**, 4613.
31 M. Kaupp, V. G. Malkin, O. L. Malkina and D. R. Salahub, *Chem. Phys. Lett.*, 1995, **235**, 382.
32 A. D. Becke, *Phys. Rev. A*, 1988, **38**, 3098.
33 J. P. Perdew, *Phys. Rev. B*, 1986, **33**, 8822; erratum 1986, **34**, 7406.
34 C. Møller and M. S. Plesset, *Phys. Rev.*, 1934, **46**, 618.
35 K. Raghavachari, G. W. Trucks, J. A. Pople and M. Head-Gordon, *Chem. Phys. Lett.*, 1989, **157**, 479.
36 (*a*) M. Dolg, U. Wedig, H. Stoll and H. Preuß, *J. Chem. Phys.*, 1987, **86**, 866; (*b*) D. Andrae, U. Häußermann, M. Dolg, H. Stoll and H. Preuß, *Theor. Chim. Acta*, 1990, **77**, 123.
37 (*a*) T. Leininger, A. Berning, A. Nicklass, H. Stoll, H.-J. Werner and H.-J. Flad, *Chem. Phys.*, 1997, **217**, 19; (*b*) www. theochem.uni-stuttgart.de and private communication H. Stoll, Stuttgart. From the original uncontracted (12s12p8d) basis set for Tl, the outermost diffuse s and p functions were deleted. The innermost six s, six p and five d primitives were contracted to represent the doubly occupied $5s^2\ 5p^6\ 5d^{10}$ orbitals with a HF calculation on the Tl^{3+} ion.
38 (*a*) W. J. Hehre, R. Ditchfield and J. A. Pople, *J. Chem. Phys.*, 1972, **56**, 2257; (*b*) P. C. Hariharan and J. A. Pople, *Theor. Chim. Acta*, 1973, **28**, 213.
39 T. H. Dunning, *J. Chem. Phys.*, 1971, **55**, 716.
40 T. H. Dunning, *J. Chem. Phys.*, 1989, **90**, 1007.
41 M. J. Frisch, G. W. Trucks, H. B. Schlegel, P. M. W. Gill, B. G. Johnson, M. A. Robb, J. R. Cheeseman, T. Keith, G. A. Petersson, J. A. Montgomery, K. Raghavachari, M. A. Al-Laham, V. G. Zakrzewski, J. V. Ortiz, J. B. Foresman, J. Cioslowski, B. B. Stefanov, A. Nanayakkara, M. Challacombe, C. Y. Peng, P. Y. Ayala, W. Chen, M. W. Wong, J. L. Andres, E. S. Replogle, R. Gomperts, R. L. Martin, D. J. Fox, J. S. Binkley, D. J. Defrees, J. Baker, J. P. Stewart, M. Head-Gordon, C. Gonzalez and J. A. Pople, GAUSSIAN94, Gaussian, Inc., Pittsburgh, PA, 1995.
42 M. J. Frisch, G. W. Trucks, H. B. Schlegel, G. E. Scuseria, M. A. Robb, J. R. Cheeseman, V. G. Zakrzewski, J. A. Montgomery, Jr., R. E. Stratmann, J. C. Burant, S. Dapprich, J. M. Millam, A. D. Daniels, K. N. Kudin, M. C. Strain, O. Farkas, J. Tomasi, V. Barone, M. Cossi, R. Cammi, B. Mennucci, C. Pomelli, C. Adamo, S. Clifford, J. Ochterski, G. A. Petersson, P. Y. Ayala, Q. Cui, K. Morokuma, D. K. Malick, A. D. Rabuck, K. Raghavachari, J. B. Foresman, J. Cioslowski, J. V. Ortiz, B. B. Stefanov, G. Liu, A. Liashenko, P. Piskorz, I. Komaromi, R. Gomperts, R. L. Martin, D. J. Fox, T. Keith, M. A. Al-Laham, C. Y. Peng, A. Nanayakkara, C. Gonzalez, M. Challacombe, P. M. W. Gill, B. Johnson, W. Chen, M. W. Wong, J. L. Andres, C. Gonzalez, M. Head-Gordon, E. S. Replogle and J. A. Pople, GAUSSIAN98, Gaussian, Inc., Pittsburgh, PA, 1998.
43 ACES II is a package of *ab initio* programs written, see J. F. Stanton, J. Gauss, J. D. Watts, W. J. Lauderdale and R. J. Bartlett, *Int. J. Quantum Chem. Symp.*, 1992, **26**, 879.
44 INTDER95 is a general program developed by Wesley D. Allen (Stanford University, 1995) which performs various vibrational analyses and higher-order nonlinear transformations among force field representations. At the harmonic level, the transformations are elementary and involve standard B-matrix techniques, see *e.g.* (*a*) G. Fogarasi and P. Pulay, in *Vibrational Spectra and Structure*, ed. J. R. Durig, Elsevier, Amsterdam, 1985, vol. 14, pp. 148–152; (*b*) E. B. Wilson, Jr., J. C. Decius and P. C. Cross, *Molecular Vibrations*, McGraw-Hill, New York, 1955; (*c*) S. Califano, *Vibrational States*, Wiley, New York, 1976.
45 (*a*) A. H. Schwellnus, L. Denner and J. C. A. Boeyens, *Polyhedron*, 1990, **9**, 975; (*b*) A. Kawamoto, J. Tanaka, A. Oda, H. Mizumura, I. Murata and K. Nakasuji, *Bull. Chem. Soc. Jpn.*, 1990, **63**, 2137; (*c*) A. L. Balch, M. M. Olmstead, P. E. Reedy and S. P. Rowley, *Inorg. Chem.*, 1988, **27**, 4289.
46 R. C. Seccombe and C. H. L. Kennard, *J. Organomet. Chem.*, 1969, **18**, 243.
47 M. Adelhelm, W. Bacher, E. G. Höhn and E. Jacob, *Chem. Ber.*, 1991, **124**, 1559.
48 F. A. Cotton and C. S. Kraihanzel, *J. Am. Chem. Soc.*, 1962, **84**, 4432.
49 (*a*) A. E. Reed, R. B. Weinstock and F. Weinhold, *J. Chem. Phys.*, 1985, **83**, 735; (*b*) A. E. Reed, L. A. Curtiss and F. Weinhold, *Chem. Rev.*, 1988, **88**, 899.
50 (*a*) M. J. S. Dewar, *Bull. Soc. Chim. Fr.*, 1951, **18**, C71; (*b*) J. Chatt and L. A. Duncanson, *J. Chem. Soc.*, 1953, 2939.
51 J. A. Pople, P. M. W. Gill and N. C. Handy, *Int. J. Quantum Chem.*, 1995, **56**, 303.
52 For example, UCCSD(T)/ECP2 yields reaction energies of +115.9, +91.5, −129.2, +71.3, −76.5, and −3.4 kcal mol^{-1} for (1)–(6), respectively. Note that the UCCSD(T)/ECP1 geometry has been used for $[Tl(CO)]^{2+}$ which is not a minimum at UCCSD(T)/ECP2.
53 The optimized transition structures are linear and have one imaginary frequency. BP86/ECP1: Tl–C^1 = 2.519 Å, Tl–C^2 = 3.167 Å, C^1–O^1 = 1.136 Å, C^2–O^2 = 1.139 Å, S^2 = 0.299. BP86/ECP2: Tl–C^1 = 2.492 Å, Tl–C^2 = 3.178 Å, C^1–O^1 = 1.124 Å, C^2–O^2 = 1.127 Å, S^2 = 0.306.

Paper 9/04709C